JACS
JOURNAL OF THE AMERICAN CHEMICAL SOCIETY

Article

Enzymatically-Degassed Surface Initiated ATRP with Real-Time Monitoring

Luis Navarro, Alan Enrique Enciso, Krzysztof Matyjaszewski, and Stefan Zauscher

J. Am. Chem. Soc., **Just Accepted Manuscript** • Publication Date (Web): 23 Jan 2019

ACS Publications

is published by the American Chemical Society. 1155 Sixteenth Street N.W., Washington, DC 20036

Enzymatically-Degassed Surface-Initiated ATRP with Real-Time Monitoring

Luis A. Navarro[1], Alan E. Enciso[2], Krzysztof Matyjaszewski[2], Stefan Zauscher[1,]*

[1]Department of Mechanical Engineering and Materials Science, Duke University, 101 Science Drive, Durham, North Carolina, 27708, United States

[2]Department of Chemistry, Carnegie Mellon University, 4400 Fifth Avenue, Pittsburgh, PA, 15213, United States

KEYWORDS: Glucose oxidase, non-fouling, antifouling, QCM, polymer brush, SIP

Abstract

Polymer brush coatings are frequently prepared by radical polymerization, a notoriously oxygen sensitive process. Glucose oxidase (GOx) can inexpensively enable radical polymerization in solution by enzymatically consuming oxygen as it oxidizes glucose. Here, we report the growth of polymeric brushes using GOx-assisted atom transfer radical polymerization (ATRP) from a surface while open to air. Specifically, we grew a set of biomedically-relevant polymer brushes, including poly(oligo(ethylene glycol)

methacrylate) (POEGMA), poly(2-dimethylaminoethyl methacrylate) (PDMAEMA), poly(sulfobetaine methacrylate) (PSBMA), and poly(2-(methylsulfinyl)ethyl acrylate (PMSEA). For each of these polymers, we monitored GOx-assisted and GOx-free ATRP reaction kinetics in real time using quartz crystal microbalance (QCM) and verified findings with localized surface plasmon resonance (LSPR). We modeled brush growth kinetics considering bimolecular termination. This model fit our data well (r^2 > 0.987 for all samples) and shows the addition of GOx increased effective kinetic chain lengths, propagation rates, and reproducibility. We tested the antifouling properties of the polymer brush coatings against human blood plasma and were surprised to find that coatings prepared with GOx repelled more plasma proteins in all cases than their GOx-free counterparts.

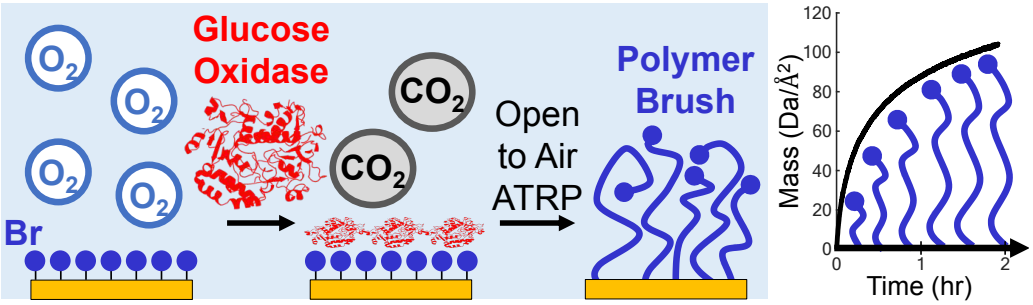

(****TOC image to be displayed in the abstract of the main paper****)

Introduction

Polymer brushes are used as surface coatings in many applications to endow an interface with a variety of useful properties, such as biocompatibility,[1] lubrication,[2]

colloidal stabilization,[3] and protein-resistance.[4] Fouling resistance is especially important for both biomedical devices[4-5] and marine applications.[6] While a variety of methods are employed to prepare polymer brushes, controlled radical polymerization techniques are especially attractive because of their high functional group tolerance and compatibility with organic and aqueous media.[7-8] In particular, atom transfer radical polymerization (ATRP) is extremely versatile for making a variety of well-defined polymeric architectures.[9-12]

However, conventional ATRP is sensitive to oxygen, leading to the development of a new ATRP technique in which activators are regenerated by electron transfer (ARGET). In ARGET ATRP, the activating Cu(I) species is formed in situ with reducing agents, such as tin(II) octoate or *L*-ascorbic acid (LAscA), which reduce oxygen-insensitive Cu(II) catalyst complexes to the Cu(I) activators.[13-14] In ARGET ATRP, an excess of reducing agent is used to reduce all initially added Cu(II) as well as any Cu(II) that accumulates following radical termination. As Cu(I) species scavenge oxygen, ARGET ATRP can be used in non-degassed solutions and still efficiently produce polymeric brushes.[15] However, polymerization kinetics can vary considerably in non-degassed mixtures,[16] leading to highly variable brush thickness. Thus, the search for new methods to perform surface-initiated ATRP (SI-ATRP) without degassing continues.[15, 17-18]

Glucose oxidase (GOx) is an enzyme that oxidizes glucose, consuming oxygen in the process (see **Scheme 1**).[19-20] Recently, several groups have reported that the reaction

between GOx and glucose can be exploited to enzymatically degas a radical polymerization medium, removing any oxygen that can deactivate growing radicals.[17, 21-23] GOx is attractive because it is an inexpensive enzyme that maintains activity in the presence of organic solvents,[24-25] and thus enables RAFT polymerizations in 70% dioxane,[21] 20% methanol,[21] and 94 proof gin.[22] Unfortunately, GOx produces hydrogen peroxide as a side product that can interfere with polymerization by initiating new chains. This interference is exacerbated in ATRP by a Fenton-like reaction with the copper activators. To address this, Enciso et al. reported that the addition of sodium pyruvate consumed the peroxide and allowed GOx-assisted ATRP reactions to achieve high, predictable molecular weights.[17] While these studies demonstrated GOx-assisted polymerizations in solution phase, enzymatic degassing for surface-initiated polymerizations (SIP) has yet to be explored. Therefore, we investigated the potential of GOx to enable SIP reactions that are typically air sensitive.

SIP kinetics are most frequently studied by ellipsometry or AFM.[7] As it is impractical to continuously follow the progress of air-free polymerizations with these techniques, kinetic studies are normally limited to a few periodic measurements of brush height. The oxygen compatibility of GOx-assisted ATRP make it uniquely suited for techniques that can continuously monitor SIP kinetics. One such technique is quartz crystal microbalance (QCM) monitoring, which has been used to follow SIP kinetics in real-time.[26-29] In a QCM experiment, a thin quartz crystal's vibrational modes are excited, and its resonant

frequencies are measured. The addition of mass to the crystal surface lowers its resonant frequency as described by the Sauerbrey[30] or Parlak equations.[31] When a polymer brush is grown from the crystal surface, the relationship between frequency and mass can be exploited to measure brush growth in real time.[32-37]

Although QCM offers a remarkable degree of time resolution for SIP kinetics, previous studies have only applied living polymerization models[38-39] even when data clearly showed severe nonlinearity.[40] Furthermore, several studies required a special setup to feed degassed polymerization mixture into a QCM chamber,[38, 40] but still suffered from variability attributed to trace oxygen.[40] As GOx-assisted ATRP does not require air-free reaction conditions, it dramatically simplifies the continuous monitoring of SIP kinetics with techniques such as QCM and localized surface plasmon resonance (LSPR). To our knowledge, LSPR has not yet been used to monitor SIP.

In this paper, we use QCM and LSPR to monitor GOx-assisted ARGET ATRP of polymer brushes that resist protein adsorption. Specifically, we compare GOx-assisted and GOx-free polymerizations by measuring brush growth over time for four different polymers: poly(oligo(ethylene glycol) methyl ether methacrylate) (POEGMA), poly(2-dimethylaminoethyl methacrylate) (PDMAEMA), poly(sulfobetaine methacrylate) (PSBMA), and poly(2-(methylsulfinyl)ethyl acrylate (PMSEA). We exploit the high temporal resolution of QCM and LSPR to study the kinetics of these reactions, and we use models accounting for bimolecular termination to fit data more accurately than in previous

studies. By examining how the polymer brushes dissipate vibrational energy, we draw inferences about adsorbed GOx during polymerization. Additionally, we test the antifouling ability of the brush coatings, finding the addition of GOx to improve protein resistance in all cases. We provide additional characterization by ellipsometry, contact angle goniometry, FTIR, and XPS to complement our findings. We show that the addition of GOx makes ARGET ATRP a more robust technique for preparing a variety of polymer brushes in the presence of air.

Experimental

Materials. This listing only shows materials used in procedures highlighted in this document. For a comprehensive list, see **Supporting Information**. Acetone (99.5%, Sigma-Aldrich), alumina (basic, 150 mesh, Sigma-Aldrich), *L*-ascorbic acid (99%, Sigma-Aldrich), blood plasma (human, lyophilized, Sigma-Aldrich), bovine serum albumin (Sigma-Aldrich), copper (II) bromide ($CuBr_2$, anhydrous, 99%, Acros), ethanol (EtOH, absolute, KOPTEC), α-*D*-glucose (96%, Sigma-Aldrich), 1,1,4,7,10,10-hexamethyl-triethylenetetramine (HMTETA, 97%, Sigma-Aldrich), hydrogen peroxide (35%, BDH Chemicals, for piranha), glucose oxidase (GOx, from *Aspergillus niger*, Sigma-Aldrich), isopropyl alcohol (IPA, 99.5%, BDH Chemicals), 2-(*N*-3-sulfopropyl-*N*,*N*-dimethyl ammonium)ethyl methacrylate (SBMA, DMAPS, 97%, Sigma-Aldrich), methanol (MeOH, 99.8%, EMD Millipore Corporation), potassium chloride (99.995 %, Alfa Aesar), potassium phosphate monobasic (99.8 %, J.T. Baker), sodium bromide (NaBr, 99%, Sigma-Alrdich), sodium chloride (99%, Macron Chemicals), sodium dodecyl sulfate (SDS, 99%, Sigma-Aldrich), sodium phosphate dibasic (99%, Sigma-Aldrich), sodium pyruvate (99%, Sigma-Aldrich), sulfuric acid (93-98%, BDH Chemicals), and tris(2-pyridylmethyl)amine (TPMA, 98%, KOEI Chemical Co.) were purchased and used as received.

Oligo(ethylene glycol) methyl ether methacrylate (OEGMA, M_n = 300 Da, Sigma-Aldrich) and 2-(dimethylamino)ethyl methacrylate (DMAEMA, 98%, Sigma-Aldrich) were passed through basic alumina to remove inhibitor and used within three hours prior to

any polymerization. PBS-Br was prepared as PBS (phosphate buffered saline), except NaCl was replaced with NaBr to form copper to bromide salts rather than chloride. The GOx-POEGMA hybrid was produced by coupling an ATRP initiator to GOx by NHS ester chemistry followed by ATRP. The hybrid's structure was determined by NMR, the POEGMA molar mass was measured by GPC, and its enzymatic activity was determined by colorimetric assay. BIBOED (disulfide ATRP initiator), MSEA (DMSO-mimicking acrylate), GOx-POEGMA hybrid, and PBS-Br were prepared with full synthetic procedures and spectra available in **Supporting Information**. Water used was Milli-Q grade and obtained using a NANOpure Diamond water purification system (Barnstead, 18.2 MΩ•cm) and filtered through a 0.22 µm Millipak 40 Gamma Gold (Millipore) filter.

Instrumentation. For details on chemical characterization, ellipsometry, contact angle goniometry, and x-ray photoelectron spectroscopy, see **Supporting Information**.

Quartz Crystal Microbalance (QCM). QCM data was measured on a QSense E4 (Biolin Scientific) with a temperature controller with a steady flow rate maintained by an IPC multichannel dispenser (model ISM935C, ISMATEC). QCM samples were prepared on 5 MHz gold-coated quartz sensor (QuartzPro). QCM data was acquired using QSoft401 (v2.5.33.748), exported with QTools (v3.1.25.604), and analyzed using a MATLAB (R2018a, v9.4.0.813654) script.

Localized Surface Plasmon Resonance (LSPR). LSPR data was obtained using an Open SPR instrument (model REV3.0, Nicoya Lifesciences) using OpenSPR software

(v3.10.6655.20567). LSPR data was analyzed using the MATLAB Curve Fitting Toolbox (v3.5.7, MATLAB R2018a, v9.4.0.813654).

Highlighted Procedures

Preparation of ATRP-initiator Surfaces. Gold-coated QCM sensors (5 MHz) were rinsed and sonicated (with 1% SDS, H_2O, acetone, and EtOH), cleaned with piranha solution, cleaned by oxygen plasma, and immersed into a 0.1% m/v solution of BIBOED initiator in ethanol at room temperature for at least 20 hours. LSPR sensors (50 nm gold nanoparticles, Nicoya Lifesciences, 9 nm EM decay length) were similarly prepared, but omitting sonication. Detailed procedures are available in the **Supporting Information**. Sensors were checked by ellipsometry and contact angle to ensure consistent and clean surfaces.

Preparation of polymerization solutions. To offer controls with matched concentrations, polymerization mixtures were prepared as combinations of a 2x glucose mixture and 2x monomer mixture (see details below). Polymerization mixtures lacking a given reagent (i.e., LAscA) had the relevant stock solution(s) replaced with an equivalent volume of solvent. All solutions were prepared volumetrically using stock solutions of reagents in PBS-Br unless otherwise noted. Solutions were not degassed and were left completely open to atmosphere throughout the polymerization, with the exception of DMAEMA, which was lightly covered with foil to prevent inhalation of the toxic monomer.

2x Glucose Mixture. A 30% glucose stock was prepared using α-*D*-glucose, which tautomerizes to β-*D*-glucose in aqueous solution. A 2x solution (50 mL) was prepared by mixing 26 mL of PBS-Br, 12 mL of 30% glucose (final 2x conc. 72 mg/mL, 400 mM, 2 eq), 11 mL of 10% sodium pyruvate (final 2x conc. 22 mg/mL, 200 mM, 1 eq), and 1 mL of 5.0 kU/mL GOx (final 2x conc. 100 U/mL, 37 mg/mL). GOx-free samples had the GOx solution replaced with an equivalent volume of PBS-Br. For the GOx-POEGMA sample, the GOx in the mixture was replaced with an equivalent volume of GOx-POEGMA (final 2x conc. 162 mg/mL), and it was compared alongside 155 kU/g GOx used as a precursor for the hybrid.

2x POEGMA Mixture. A 2x mixture (50 mL) was prepared by mixing 25 mL of PBS-Br, 17.6 mL of OEGMA (M_n = 300 Da, final 2x conc. 0.369 g/mL, 1.232 M, 1166 eq), 1.18 mL of 10 mg/mL $CuBr_2$ (final 2x conc. 0.236 mg/mL, 1.06 mM, 1 eq), 19.8 mg HMTETA (final 2x conc. 0.396 mg/mL, 1.72 mM, 1.6 eq), and *L*-ascorbic acid (added last, approx. 5 min prior to polymerization). For 20xAA conditions, 6.2 mL of 30 mg/mL *L*-ascorbic acid was used (final 2x conc. 3.76 mg/mL, 21.3 mM, 20 eq). For 0.2xAA conditions, 6.2 mL of 0.3 mg/mL *L*-ascorbic acid was used (final 2x conc. 37.6 μg/mL, 0.213 mM, 0.2 eq). *L*-ascorbic acid was added at the last possible moment (approx. 5 min prior to polymerization), causing the 20xAA mixtures to turn from medium intensity navy blue to colorless, while no such color change was observed in 0.2xAA mixtures.

2x PDMAEMA Mixture. A 2x mixture (30 mL) was prepared by mixing 15.7 mL of PBS-Br, 6.0 mL of DMAEMA (final 2x conc. 200 mg/mL, 1.18 M, 592 eq), 1.34 mL of 10 mg/mL $CuBr_2$ in MeOH (final 2x conc. 0.446 mg/mL, 2 mM, 1 eq), 34.8 mg TPMA (final 2x conc. 1.16 mg/mL, 4 mM, 2 eq), and *L*-ascorbic acid (added last, approx. 5 min before polymerization). For 20xAA conditions, 7.0 mL of 30 mg/mL *L*-ascorbic acid in MeOH was used (final 2x conc. 7.0 mg/mL, 40 mM, 20 eq). For 0.2xAA conditions, 7.0 mL of 0.3 mg/mL *L*-ascorbic acid in MeOH was used (final 2x conc. 70 µg/mL, 0.4 mM, 0.2 eq). $CuBr_2$ and TPMA were mixed for at least 10 minutes (yielding a medium intensity Kelly green soln.). The color of the copper complex did not change color upon mixing with DMAEMA, but turned cyan upon mixing with 2x glucose mixture (containing PBS-Br).

2x PSBMA Mixture. This 2x mixture was prepared as with the 2x POEGMA mixture shown above with the following change. The OEGMA was replaced with 40% SBMA stock in PBS-Br for a final 2x SBMA concentration of 0.615 M (583 eq, for 0.5x monomer conc.) or 1.23 M (1166 eq, for 1x monomer conc.).

2x PMSEA Mixture. This 2x mixture of PMSEA was prepared like the 2x PDMAEMA mixture shown above with two changes. First, the MSEA mixture replaced all MeOH with PBS-Br. Second, DMAEMA was replaced with 42% MSEA stock in PBS-Br for a final 2x MSEA concentration of 924 mM (463 eq, for 0.5x monomer conc.) or 1.85 M (925 eq, for 1x monomer conc.).

General QCM Experimental Design. Initiator-coated QCM sensors were rinsed with ethanol, blown dry with nitrogen, and loaded into a QCM chamber. The flow cells were assembled following manufacturer instructions, using PTFE tape to secure tubes, and tapping each chamber ten times on each side with a metal spatula to relieve stress on the crystal. A peristaltic pump was used to flow solution through the QCM cells at steady rate (0.1 mL/min), while the temperature of the cells was maintained at 25 ^{o}C. The frequencies of each overtone (n = 1, 3, 5, 7, 9, 11, and 13) of each sensor were found in air, then the chambers were filled with PBS-Br, and the frequencies of each overtone were found again. Overtone frequencies in PBS-Br were used for data analysis. Before starting the experiment, the flow of the peristaltic pump was repeatedly reversed (5 second delay) to check for the presence of bubbles, which typically show a reversible frequency spike when the change in flow direction sends a pressure wave through the liquid. For detailed procedures on preparing polymerization mixtures, see above. The order of solutions for the polymerizations were as follows: (1) PBS-Br, (2) 1x glucose mixture (contains glucose, sodium pyruvate, and GOx if applicable), (3) 1x glucose mixture with monomer, (4) full polymerization mixture (contains glucose, sodium pyruvate, GOx if applicable, monomer, $CuBr_2$, ligand, and *L*-ascorbic acid), (1) PBS-Br, (5) 10% plasma (8 mg/mL), (1) PBS-Br, and (6) H_2O (see **Figure 1**). For solutions where *L*-ascorbic acid or GOx were used, these reagents were added roughly 5-10 min prior to flowing a reaction solution containing

them. Plasma solutions were reconstituted from a lyophilized powder in water within 20 min of usage. For details on data analysis, see **Supporting Information**.

LSPR Experimental Design. LSPR was conducted with a similar experimental design to QCM experiments. For details, see **Supporting Information**.

Results and Discussion

Scheme 1. Schematic GOx deoxygenation [a] and surface-initiated polymerization of various monomers from initiator-modified surfaces.

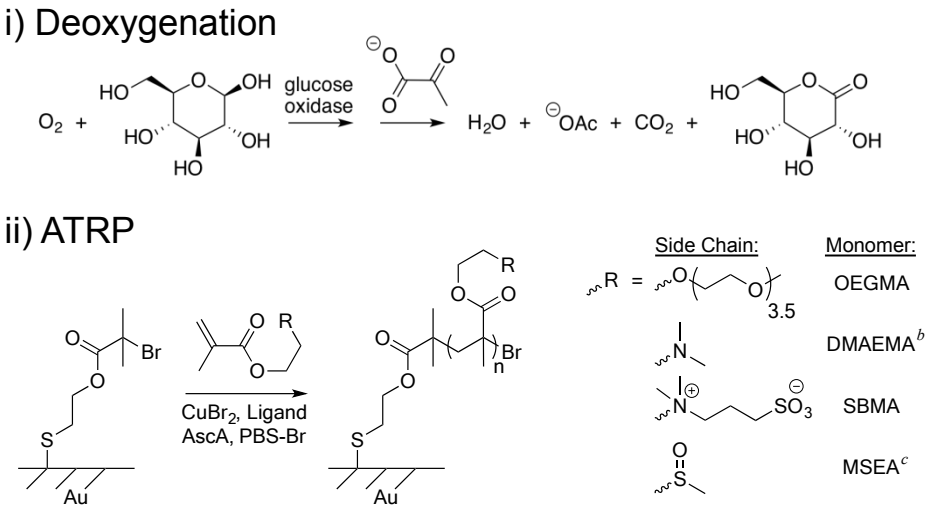

[a] First, GOx consumes oxygen to oxidize glucose, producing an undesired hydrogen peroxide side product. Second, pyruvate in solution consumes hydrogen peroxide without the aid of GOx to yield CO_2, H_2O, and acetate as benign side products.

[b] DMAEMA used 50% PBS-Br, 40% MeOH, and 10% monomer.

[c] MSEA is an acrylate monomer with a slightly different backbone than the other methacrylate.

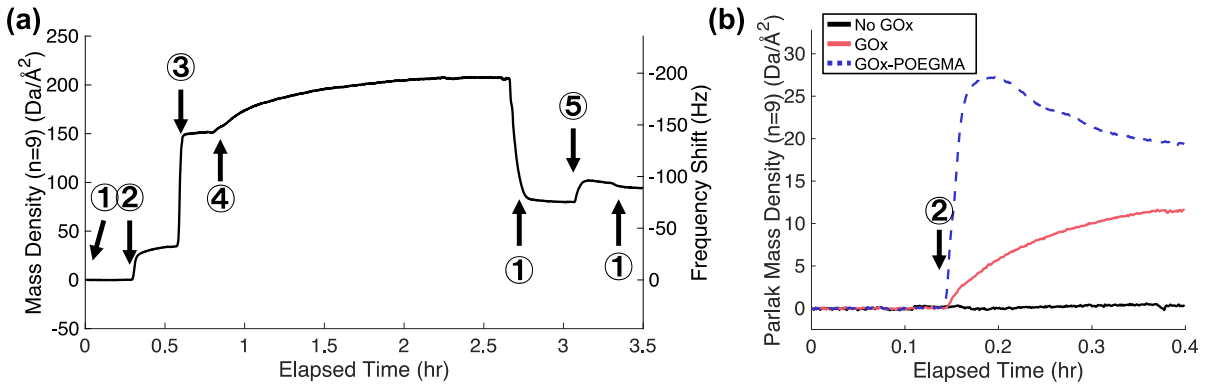

	①	②	③	④	⑤
PBS-Br (buffer)	+	+	+	+	-
Glucose, pyruvate, GOx	-	+	+	+	-
Monomer	-	-	+	+	-
$CuBr_2$, ligand, 0.2eq LAscA	-	-	-	+	-
10% Blood Plasma	-	-	-	-	+

Figure 1. General overview of polymerization experiments. (a) Mass density on a QCM sensor during a typical experiment for growing and testing a POEGMA brush grown by GOx-assisted ARGET ATRP. Mass density was calculated by the Sauerbrey equation, in which increases in fluid density and viscosity produce artificially inflated values when changing solutions. The table shows reagents in solutions flowed over the surface of an initiator-coated QCM sensor starting at the annotated points on the graph. For reference, a 1.06 Da/Å^2 corresponds to a 1 Hz drop in frequency. (b) Apparent mass density on an initiator-coated QCM sensor upon adding glucose, pyruvate, and glucose oxidase (GOx), followed by a buffer rinse (PBS-Br). Curves are shown for a glucose mixture lacking GOx (black), containing GOx (red), or containing a GOx-POEGMA hybrid (blue dash). Mass

density was calculated using the Parlak equation,[31] which corrects for fluid viscosity effects.

Polymerization Experimental Design

For this study, we chose to use ATRP for its compatibility with a broad range of monomers. Specifically, we chose the oxygen-tolerant ARGET ATRP because its oxygen tolerance can be tuned by varying the amount of reducing agent per copper. *L*-ascorbic acid (LAscA) was chosen as a reducing agent because it reduces Cu(II) species to Cu(I) with a semiquinone-like byproduct that rapidly consumes oxygen.[41-42] We compared reactions with 20 equivalents of LAscA (20-40 mM, 20xAA) which is sufficient to react with both copper and dissolved oxygen, and 0.2 equivalents (0.2-0.4 mM, 0.2xAA) which can only reduce a fraction of the copper. As all mixtures were non-degassed and completely open to air, reactions with 0.2 equiv of LAscA would require some external aid to remove dissolved oxygen (0.26 mM at STP) that hampers the polymerization by both oxidizing copper and by terminating propagating chains. In contrast, 10-20 mM of LAscA is a proven method of growing polymer brushes by ARGET ATRP in non-degassed polymerization mixtures,[15-16] although it may yield variable results.[16]

We first tested the ability of GOx to enable SIP. Briefly, we started with an initiator-coated gold surface in a QCM or LSPR flow cell and subsequently flow, in order: a GOx mixture, a GOx mixture containing monomer, a full GOx-containing polymerization mixture, buffer, 10% blood plasma, and buffer (see **Figure 1a**). This procedure distinctly

shows three major events: fouling of the clean sensor by GOx, polymerization without degassing, and the fouling of the completed polymer brush with plasma protein. The addition of protein and polymer mass can be tracked with these techniques, and the instantaneous slopes in **Figure 1a** reveal the evolving polymerization rate. In addition to QCM and LSPR, polymer brushes were characterized by contact angle, ellipsometry, FTIR-ATR, and XPS (for POEGMA) to verify brush growth and identity.

GOx reliably fouled clean sensors, as illustrated in **Figure 1b** (12.9 ± 4.8 Da/Å^2 by Parlak, 14.1 ± 4.6 Da/Å^2 by Sauerbrey, mean ± SD across 8 QCM sensors). Surprisingly, GOx fouling did not inhibit the polymerization of any of the polymers we tested (**Figure 2**). This is consistent with findings by Divandari et al., who showed PNIPAM brushes would still grow by ATRP when fouled by hemoglobin.[43]

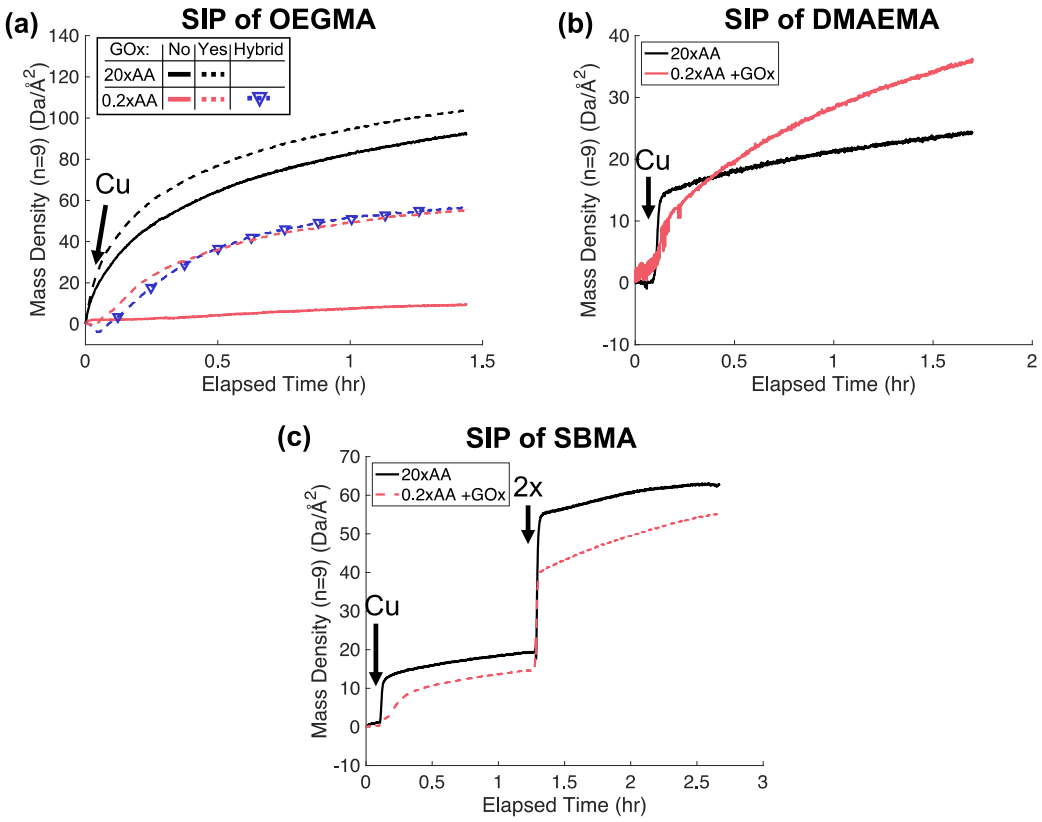

Figure 2. Sauerbrey-calculated mass densities of various polymer brushes grown from QCM crystals during ARGET ATRP with 20xAA per Cu (black) or 0.2xAA per Cu (red) in the absence of GOx (solid) or presence of GOx (dash). GOx-POEGMA-assisted ATRP with 0.2xAA (blue dash ▽) is also shown. At time t = 0, the sensors were equilibrated with glucose, pyruvate, GOx, and monomer solution (point ③ in **Figure 1a**). Annotated time points denote: (Cu) the addition of copper catalyst and reducing agent and (2x) the doubling of monomer concentration in a polymerization mixture. Plots show SIP for (a) POEGMA, (b) PDMAEMA, and (c) PSBMA.

Table 1. Compilation of QCM and spectroscopic ellipsometry measurements of polymer brushes grown from QCM crystals. The rate constants shown reflect parameters from fitting QCM data to a bimolecular termination model (mass = $k_p[M]/2k_t \ln(1+k_t I_0 t)$) based on Sauerbrey-calculated mass densities from the 9th overtone.

Polymer	LAscA/Cu	GOx	[M] (mM)	Polymer[a] (Da/Å^2)	Plasma Fouling (Da/Å^2)	$k_p[M]/2k_t$ (Da/Å^2)	k_p [M] I_0 (Da/Å^2/hr)	Ellipsometry[b] (nm)
Bare	-	No	-	-	95.2	-	-	3.8 ± 0.2
Bare	-	Yes	-	-	67.8	-	-	3.2 ± 0.1
POEGMA	20	No	620	120.2	1.4[c]	28.8	375.4	6.0 ± 0.6[c]
POEGMA	20	No	620	65.9	19.9	53.2	33.9	3.6 ± 0.1
POEGMA	20	Yes	620	139.4	-1.3[c]	26.7	637.9	8.5 ± 0.8[c]
POEGMA	0.2	No	620	24.9	6.6[c]	5.9	11.3	1.2 ± 0.2[c]
POEGMA	0.2	Yes	620	73.0	1.0[c]	13.9	336.1	5.9 ± 0.1[c]
POEGMA	0.2	Yes	620	80.2	14.2	15.7	183.4	5.6 ± 0.4
POEGMA	0.2	Yes	620	82.1	-	19.6	175.1	4.4 ± 0.3[d]
POEGMA	0.2	Hybrid	620	101.1	2.7	18.7	218.5	8.6 ± 0.2
PDMAEMA	20	No	590	32.3	32.5	7.5	11.7	2.3 ± 0.3
PDMAEMA	0.2	Yes	590	34.6	-	16.6	47.5	4.5 ± 0.1
PSBMA[e]	20	No	310	39.5	64.5	5.0	10.2	1.3 ± 0.1[d]
			620			8.2	10.7	3.0 ± 0.1
PSBMA[e]	0.2	Yes	310	45.8	50.0	6.4	7.6	2.4 ± 0.1[d]
			620			16.4	18.0	3.1 ± 0.1
PMSEA[e]	20	No	460	66.3	65.9	59.0	72.9	1.6 ± 0.1[d]
			920			9.3	25.4	3.3 ± 0.1
			460			7.4	10.7	
PMSEA[e]	0.2	Yes	460	42.3	55.8	6.0	81.1	1.2 ± 0.1[d]
			920			300.5	4.5	3.5 ± 0.1
			460			1.2	10.2	

[a]This quantity represents the total mass on the QCM crystal following polymerization, including any GOx which may be on the crystal.

[b]Ellipsometry measurements are taken after fouling with plasma unless otherwise noted, including any dry thickness which may result from polymer, GOx, and plasma. Values are shown as mean ± standard deviation resulting from three independent measurements on the same crystal.

[c]These quantities correspond to samples fouled with BSA, not plasma.

[d]These ellipsometry measurements were taken on a polymer sample that was not fouled with BSA nor plasma.

[e]PSBMA and PMSEA samples had multiple monomer concentration mixtures flow over the growing brush surface. The different monomer concentrations are listed sequentially (top to bottom) in the order they were used.

GOx Assistance in ATRP of POEGMA

We first tested polymerizations with POEGMA because it is well controlled in ATRP[44] and it is an antifouling polymer (**Figure 2a**). ATRP with 20xAA was mildly accelerated by GOx even though GOx was not needed to fully remove oxygen. With only 0.2 equiv of LAscA, GOx-assistance was necessary for the reaction to proceed at a reasonable rate. Based on the higher observed rates of brush growth, we concluded that GOx provides beneficial degassing of the reaction mixture and that GOx fouling does not significantly impair polymerization. This holds true regardless of the amount of reducing agent added. Furthermore, both the shapes of the growth curves and the values of fit rate constants were more consistent across duplicate experiments for polymerizations using GOx with 0.2xAA than for GOx-free with 20xAA. From this, we conclude that GOx activity leads to more reproducible open-to-air polymerizations.

We also investigated the effect of using a GOx-POEGMA biohybrid instead of GOx to perform this polymerization. We expected this modification to reduce GOx fouling to

allow us to observe the degassed polymerization without surface-active GOx. However, it instead caused more mass to adsorb commensurate with its higher molar mass (**Figure 1b**). Furthermore, using a colorimetric assay, we found the POEGMA modification nearly extinguished the hybrid's enzymatic activity (0.2% remaining activity). Despite its greatly reduced activity, the modified enzyme still produced SIP kinetics similar to that of native GOx. This implies only a small amount of GOx activity is actually necessary to assist SI-ATRP. Furthermore, a small mass loss (~4 Da/Å^2) is observed in the first two minutes of the reaction, a feature observed to a lesser degree with the lighter native GOx (**Figure 2a**). This implies that GOx-assisted SIP of POEGMA starts with some desorption of GOx. As adsorbed GOx is still observed immediately before the addition of catalyst (see **Figure S1**), we conclude that GOx desorption was induced by the formation of a POEGMA brush beneath it.

GOx-Assisted ATRP of Other Polymer Brushes

Following successful GOx-assisted ATRP of OEGMA, we tested this technique with other monomers. We preserved the (meth)acrylate functionality and focused on two ATRP conditions using 20xAA (GOx-free) and GOx-assisted 0.2xAA. Because POEGMA growth caused GOx desorption, we wanted to challenge the reaction with a polymer brush that could prevent GOx desorption. Thus, we tested PDMAEMA, a polycation known for fouling BSA.[45] GOx-assisted 0.2xAA ATRP produced a thicker PDMAEMA brush than unassisted 20xAA ATRP (**Figure 2b**). Furthermore, GOx assistance also leads to a more even

polymerization rate of DMAEMA throughout brush growth, showing that GOx is beneficial even with fouling polymers.

To further explore the variety of polymers amenable with GOx, we similarly produced PSBMA (poly(sulfobetaine methacrylate)), an antifouling polyzwitterion (**Figure 2c**). Similar to the case of DMAEMA, GOx led to more even growth rates of SBMA throughout the reaction. We also tested poly(2-(methylsulfinyl)ethyl acrylate) (PMSEA), a DMSO-mimicking acrylic polymer with promise in biomedical applications.[46] However, this polymerization suffered from monomer-specific challenges even for GOx-free ATRP.

Polymerization Kinetics

QCM and LSPR offer a unique way to continuously follow the progress of surface-initiated polymerizations. These real-time monitoring techniques excel at providing much more detailed information on polymerization by revealing subtle changes in polymerization rate caused by phenomena such as termination. While this is not the first study to show SIP in real time, it is the first study to take full advantage of the high temporal resolution offered by these methods to examine non-linear growth kinetics during polymerization. Furthermore, their high resolution make it possible to accurately distinguish polymerization from simultaneously occurring GOx desorption. Our reactions conditions are appropriate for testing the limits of QCM and LSPR for monitoring SIP.

QCM data show that all brush growth curves were concave down (i.e., decreasing slope) regardless of the presence of GOx. Since fresh reagent mixture was flowed over the surface throughout the reaction, this observation indicates a gradual slowdown of polymerization caused

by termination (**Figure 2**). Thus, we fit the kinetics of these reactions following a model that accounts for bimolecular termination,

$$X_n(t) = \frac{k_p[M]}{2k_{t2}} \ln\left(1 + 2k_{t2} I_0\, t\right),$$

where X_n is the number average degree of polymerization within the polymer brush (proportional to areal mass density), k_p is the propagation rate, $[M]$ is the monomer concentration, k_{t2} is the bimolecular termination rate constant, and I_0 is the starting active initiator area density. We compared this model to unimolecular termination by a constant concentration of dissolved oxygen,

$$X_n(t) = \frac{k_p[M]I_0}{k'_{t1}}\left(1 - \mathrm{e}^{-k'_{t1}t}\right),$$

where k_{t1}' is the effective unimolecular termination rate constant times oxygen concentration. For full derivations for both models, see **Supporting Information: Derivations**. For representative fits, see **Figure 3**. For all fits, see **Figures S19, S26, S30, and S33**.

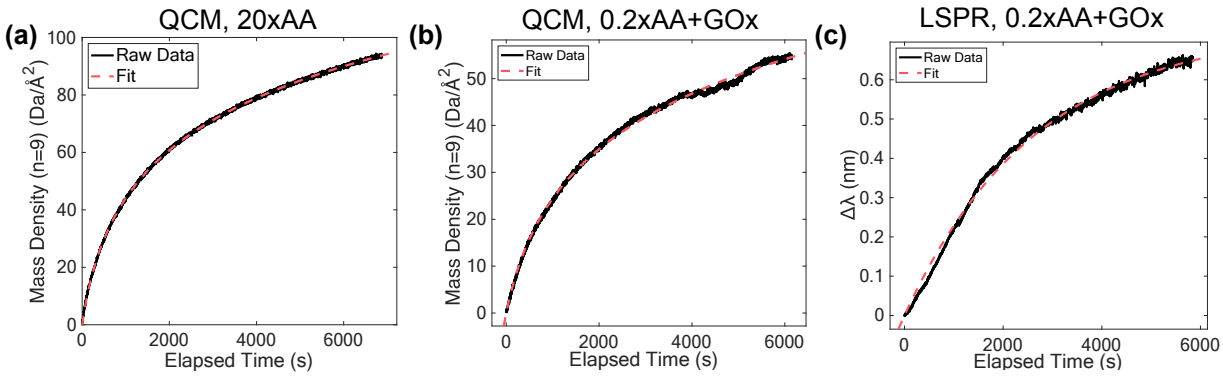

Figure 3. Kinetic fits of representative polymerizations of POEGMA with raw data (black) and fits (red, dash). (a,b) show Sauerbrey-calculated mass densities from QCM data fit to a bimolecular termination model ($m = A \ln(1+B t)$). (a) ARGET ATRP of POEGMA on QCM with 20xAA. (b) GOx-assisted ATRP of POEGMA on QCM with 0.2xAA. For fit values, see **Table 1**. (c) LSPR data of POEGMA grown by GOx-assisted ARGET ATRP with 0.2xAA fit to a living polymerization model ($\Delta\lambda = A (1-\exp(-B t))$), yielding A = 0.7299 nm and B = $3.762*10^{-4}$ s^{-1}. See **Supporting Information** for derivations.

Both termination models fit QCM data accurately ($r^2 > 0.97$). At longer times, the difference between the two models is that a brush undergoing bimolecular termination grows at a continuously slowing rate (as a log), while a brush undergoing unimolecular termination approaches a plateau (as an exponential). However, drift inherent to QCM prevents one from distinguishing between these models at those later times. In QCM, frequency may drift by a few Hz per hour due to thermal drift or changes in polymer swelling. Therefore, once the polymerization has slowed significantly, it becomes difficult to discriminate between the two termination mechanisms. For our analysis, we will focus on bimolecular termination due to more consistent fit results and prior work.[47]

To test the validity of the bimolecular termination model for our SIP reactions, we analyzed the parameters obtained from our fits. Specifically, we looked at the effective kinetic chain lengths, k_p [M]/k_{t2}, which are independent of the fraction of dead chains. First, we observe that duplicate polymerizations of OEGMA have very different kinetic

chain lengths in the absence of GOx. In contrast, hybrid-assisted and duplicate GOx-assisted polymerizations show quantitatively consistent results, i.e., k_p[M]/k_{t2} varies with 18% relative deviation. Furthermore, we grew PSBMA and PMSEA by sequentially flowing polymerization mixtures of doubled monomer concentration over the same surfaces to test that the fit-derived effective kinetic chain length is proportional to monomer concentration. Doubling monomer concentration for PSBMA increased effective kinetic chain length by 62% (20xAA) and 154% (0.2xAA, GOx-assisted). This result is within error of the expected increase of 100% $\pm$ 50% (S.D. after error propagation). Kinetic results for MSEA are more consistent with a non SI-ATRP growth mechanism. With the exception of PMSEA, all the tested polymerizations yielded consistent results under a bimolecular termination model. Despite this, further study using variable initiator surface density is necessary to clearly distinguish between unimolecular and bimolecular termination.

To complement QCM results, we repeated GOx-assisted, 0.2xAA ARGET ATRP in an LSPR (**Figure 3c**). Where QCM detects a growing polymer brush through acoustic waves, LSPR gives complementary measurements by probing a polymer brush through its optical properties. LSPR successfully detected POEGMA growth during GOx-assisted ATRP, confirming QCM results (see **Supporting Information** for formulas and fits).

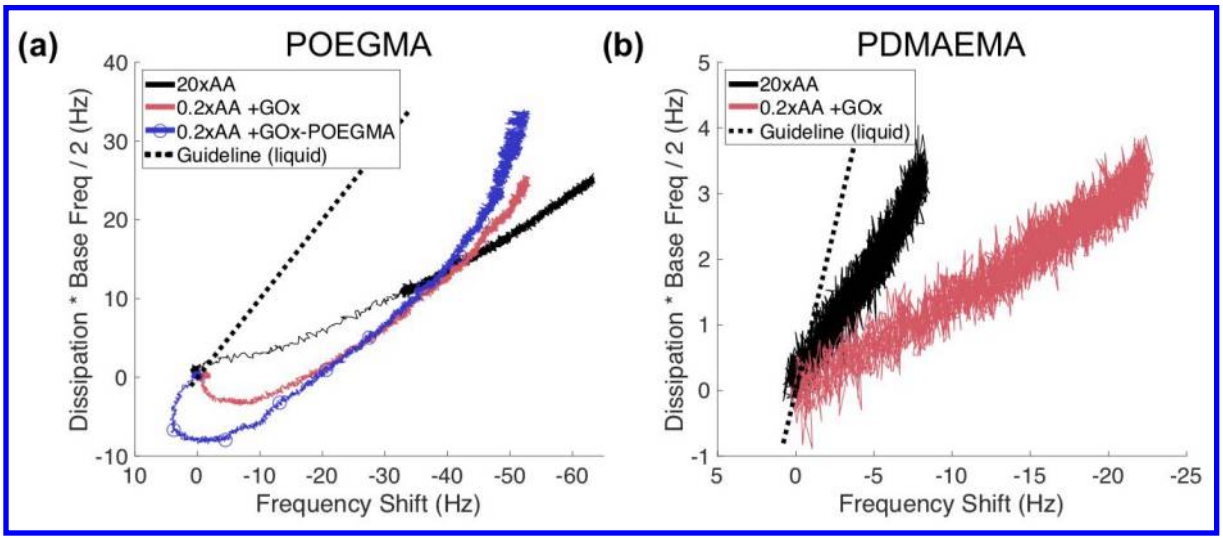

Figure 4. Evolution of normalized dissipation versus frequency drop during the growth of (a) POEGMA and (b) PDMAEMA brushes. Conditions are shown for 20xAA (black), 0.2xAA with GOx (red), and 0.2xAA with GOx-POEGMA (blue, O). For reference, a guideline (black dot) is shown for the slope that corresponds to pure fluid viscosity. We note that frequency drop (abscissa) is directly proportional to polymer brush mass density.

Brush Properties

Both QCM and LSPR give additional information about polymer brush properties beyond kinetics and fouling. For example, by fitting LSPR data, we determined a swollen POEGMA brush to be 5.1% v/v POEGMA, which is consistent with the 4.0% volume fraction measured by liquid ellipsometry. Furthermore, by analyzing dissipation versus frequency in QCM data, it is possible to identify changes in energy dissipation per unit mass of polymer brush during polymerization (**Figure 4**). In this plot, the growth of a thin, homogeneous polymer layer would produce a straight line of reproducible slope that is characteristic of the layer's dissipation per unit mass. GOx-free POEGMA growth follows this

type of linear trend (**Figure 4a**). In contrast, GOx and GOx-POEGMA assisted ATRP both show large downward hooks in the dissipation vs. frequency plot at the start of polymerization. The backward slope in this distinctive feature indicates mass loss at the start of polymerization, followed by a downward slope that reveals initial stiffening of the adsorbed layer. The mass loss is associated with GOx desorption from the surface. As polymerization progresses, GOx and GOx-POEGMA produce curves with an upward concavity (i.e., increasing slope), which indicates a gradual increase in dissipation/mass throughout the growth process. In the case of PDMAEMA, GOx leads to substantially stiffer brushes that dissipate 60% less energy per unit mass than GOx-free PDMAEMA (**Figure 4b**). This suggests GOx intimately integrates into the PDMAEMA, consistent with observations of BSA being entrapped in PDMAEMA.[45]

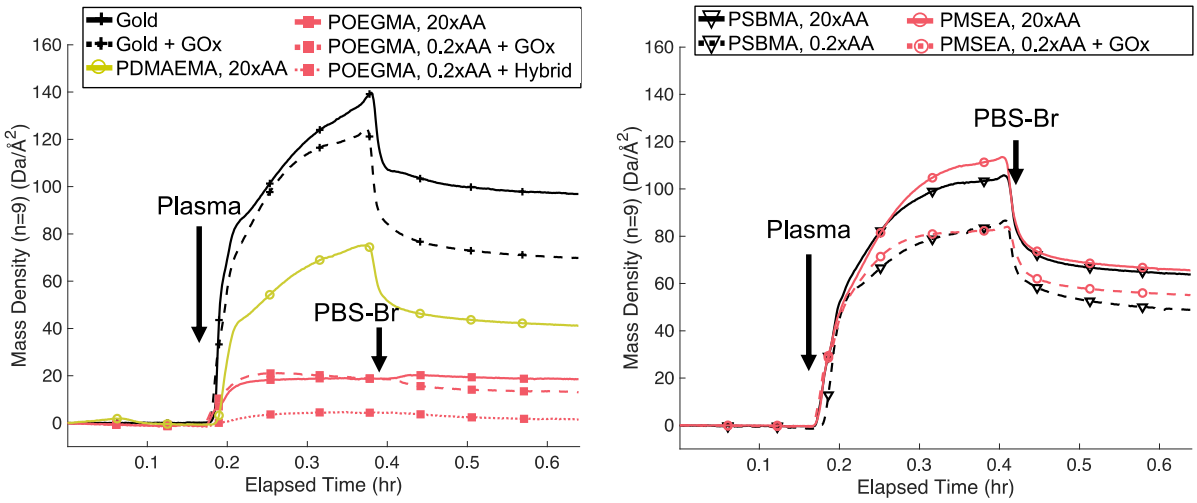

Figure 5. Fouling of polymer-coated QCM sensors by plasma. Times indicated by arrows denote exposure to 10% human blood plasma and rinsing with PBS-Br buffer. The various lines denote: (black, +, solid) initiator-coated gold without polymer, (black, +, dash) initiator-coated gold previously coated with GOx, (red, ■) POEGMA brushes, (yellow, ○)

PDMAEMA brushes, (black, ▽) PSBMA brushes, and (red, ○) PMSEA brushes. Line styles denote surfaces prepared by ATRP with: (solid) 20xAA without GOx, (dash) 0.2xAA with GOx, and (dot) 0.2xAA with GOx-POEGMA. Mass densities are calculated from the QCM sensors' 9th mode using the Sauerbrey equation.

Plasma Fouling

One could envision GOx fouling to produce patches where polymers do not grow, decreasing the quality of polymer coatings made by GOx-assisted SIP. Thus, we tested the antifouling capabilities of brushes prepared with and without GOx because patches could serve as sites for fouling. We first tested fouling by exposing various POEGMA coatings to 1% BSA solution and measuring any adsorbed mass by QCM (**Table 1**). The addition of GOx or high amounts of reducing agent (20xAA) were both effective measures for producing BSA-resistant polymer coatings. However, the coating prepared without GOx and minimal reducing agent (GOx-free 0.2xAA) appreciably fouled BSA (6 Da/Å^2). Emboldened by these results, we probed our brush coatings using 10% human blood plasma, which is a much stronger challenge for antifouling because it contains a myriad of proteins (**Figure 5**). Plasma was used at a reduced concentration (10%) to avoid potential complications with viscosity. As even 0.1% plasma will adsorb to saturation,[48] this reduced concentration should minimally impact total adsorption.

As a first control, we found that 10% plasma extensively fouled initiator-coated gold surfaces (95.2 Da/Å^2) and GOx-coated gold surfaces to a lesser extent (67.8 Da/Å^2). For the purposes of our comparisons, we kept brush thickness consistent between GOx-assisted and GOx-free samples of a given polymer. However, maintaining brush thickness between different polymer types is impractical because of differences in swelling and chain lengths. Furthermore, polymer coatings were kept thin to minimize "hearing loss" of the quartz crystals. Hearing loss is a reduction of sensitivity to adsorption on top of a thick, dissipative film that attenuates acoustic waves.[49] Despite their low film thickness, all polymer coatings repelled a significant amount of blood plasma, and GOx-assisted brushes all exhibited less fouling than their GOx-free counterparts. Similar to the bare gold surfaces, we suspect that GOx does not form vulnerable patches, but rather acts as a blocking agent for plasma, like BSA in ELISA. PSBMA and POEGMA are both known antifouling coatings, but our POEGMA samples appear far superior, likely due to thicker brush layers as seen by ellipsometry (**Table 1**). However, we note that thicker brushes may reduce apparent adsorption in QCM by both blocking adsorption and reducing sensitivity through hearing loss.

Conclusions

We demonstrated that GOx-assisted SI-ATRP is an effective and robust route for synthesizing polymer brushes. GOx rapidly consumes oxygen, which enables the open-to-air preparation of polymer brush coatings. GOx-assistance also makes non-degassed

ARGET ATRP far more reliable by reducing variability in SIP kinetics. Although GOx fouled initiating surfaces, it surprisingly did not prevent SI-ATRP of a range of monomers. Quite the opposite, the presence of GOx benefitted the polymerization of anti-fouling coatings and improved their fouling resistance. QCM and LSPR were both effective and complementary methods for monitoring polymer brush growth. However, short EM decay length limits LSPR to follow brush growth kinetics to the early stages of polymerization. QCM is effective until the rates of signal drift and brush growth become comparable in magnitude. Despite the commonly observed nonlinear brush growth kinetics, previous QCM studies only used living polymerization models. Herein, we exploited the high resolution of QCM to probe the non-negligible contribution of termination to brush growth. Furthermore, by examining plots of dissipation versus frequency, we made qualitative inferences about the stiffness of the polymer brush layers during polymerization. Lastly, antifouling coatings, most notably POEGMA, successfully reduced fouling by blood plasma.

Moreover, the oxygen tolerance provided by GOx facilitates monitoring techniques such as QCM and SPR to follow SIP kinetics in real time. In practice, these techniques can also be used to prepare sensors with well-defined brush thicknesses by indicating when to halt the polymerization to achieve a specified brush height. The inexpensive reagents and oxygen tolerance inherent to GOx-based deoxygenation enables producing antifouling brush coatings for larger-scale applications, like marine antibiofouling. While

we focused on GOx-assisted ATRP, it is likely that GOx-assistance will be compatible with a variety of other surface-initiated polymerization techniques, such as RAFT and NMP.

Associated Content

The following files are available free of charge.

Extended discussion, additional synthetic procedures, and additional sample spectra and statistics (PDF)

Derivations of kinetics models (PDF)

AUTHOR INFORMATION

Corresponding Author

zauscher@duke.edu

Present Addresses

n/a

Author Contributions

The manuscript was written through contributions of all authors. All authors have given approval to the final version of the manuscript.

Funding Sources

Funding was provided by the National Science Foundation (NSF) Triangle Materials Research Science and Engineering Center (MRSEC; DMR-1121107) for experiments at Duke University. Funding was provided by the National Science Foundation (NSF, DMR 1501324). A. E. Enciso acknowledges the Mexican Council for Science and Technology (CONACyT) for the posdoctoral award (291231-2do año de Continuidad de Estancias Posdoctorales en el Extranjero Vinculadas a la Consolidación de Grupos de Investigación).

Notes

None.

Acknowledgements

We are grateful to Yeongun Ko in Prof. Jan Genzer's group (North Carolina State University) for aiding in liquid ellipsometry measurements. We are thankful to Daniel L. French in Prof. Zauscher's group (Duke University) for supplying the disulfide initiator used in coating gold surfaces. We are grateful to Zehra Parlak for helpful discussion on interpretation of QCM results.

Abbreviations

0.2xAA, ARGET ATRP with 20 equiv of LAscA per copper; 20xAA, ARGET ATRP with 20 equiv of LAscA per copper; ARGET, activators regenerated by electron transfer; LAscA, *L*-ascorbic acid; ATRP, atom-transfer radical polymerization; BIBOED, bis[2-(2'-bromoisobutyryloxy)ethyl] disulfide (ATRP initiator); BSA, bovine serum albumin; GOx,

glucose oxidase; HMTETA, 1,1,4,7,10,10-hexamethyl-triethylenetetramine; LSPR, localized surface plasmon resonance; PBS-Br, phosphate buffered saline (with NaBr used in place of NaCl); PDMAEMA, poly(2-(dimethylamino)ethyl methacrylate); PMSEA, poly(2-(methylsulfinyl)ethyl acrylate); POEGMA, poly(oligoethylene glycol methacrylate) (monomer M_n = 300 Da for polymer brushes, M_n = 500 Da for biohybrids); PSBMA, poly(2-(*N*-3-sulfopropyl-*N*,*N*-dimethyl ammonium)ethyl methacrylate) (aka. poly(DMAPS)); QCM, quartz crystal microbalance; SPR, surface plasmon resonance; TPMA, tris(2-pyridylmethyl)amine.

References

1. Milner, S. T., Polymer brushes. *Science* **1991,** *251* (4996), 905-914.
2. Zhulina, E. B.; Rubinstein, M., Lubrication by Polyelectrolyte Brushes. *Macromolecules* **2014,** *47* (16), 5825-5838.
3. Zhao, B.; Brittain, W. J., Polymer brushes: surface-immobilized macromolecules. *Progress in Polymer Science* **2000,** *25*, 677-710.
4. Chen, S.; Li, L.; Zhao, C.; Zheng, J., Surface hydration: Principles and applications toward low-fouling/nonfouling biomaterials. *Polymer* **2010,** *51* (23), 5283-5293.
5. Krishnamoorthy, M.; Hakobyan, S.; Ramstedt, M.; Gautrot, J. E., Surface-initiated polymer brushes in the biomedical field: applications in membrane science, biosensing, cell culture, regenerative medicine and antibacterial coatings. *Chem Rev* **2014,** *114* (21), 10976-11026.
6. Callow, J. A.; Callow, M. E., Trends in the development of environmentally friendly fouling-resistant marine coatings. *Nat Commun* **2011,** *2*, 244.
7. Barbey, R.; Lavanant, L.; Paripovic, D.; Schuwer, N.; Sugnaux, C.; Tugulu, S.; Klok, H. A., Polymer brushes via surface-initiated controlled radical polymerization: synthesis, characterization, properties, and applications. *Chem Rev* **2009,** *109* (11), 5437-5527.
8. Zoppe, J. O.; Ataman, N. C.; Mocny, P.; Wang, J.; Moraes, J.; Klok, H. A., Surface-Initiated Controlled Radical Polymerization: State-of-the-Art, Opportunities, and Challenges in Surface and Interface Engineering with Polymer Brushes. *Chem Rev* **2017,** *117* (3), 1105-1318.

9. Matyjaszewski, K., Atom Transfer Radical Polymerization (ATRP): Current Status and Future Perspectives. *Macromolecules* **2012,** *45* (10), 4015-4039.
10. Matyjaszewski, K.; Tsarevsky, N. V., Macromolecular engineering by atom transfer radical polymerization. *J Am Chem Soc* **2014,** *136* (18), 6513-6533.
11. Matyjaszewski, K.; Tsarevsky, N. V., Nanostructured functional materials prepared by atom transfer radical polymerization. *Nat Chem* **2009,** *1* (4), 276-288.
12. Matyjaszewski, K., Advanced Materials by Atom Transfer Radical Polymerization. *Adv Mater* **2018,** *30* (23), e1706441.
13. Matyjaszewski, K.; Jakubowski, W.; Min, K.; Tang, W.; Huang, J.; Braunecker, W. A.; Tsarevsky, N. V., Diminishing catalyst concentration in atom transfer radical polymerization with reducing agents. *Proc Natl Acad Sci U S A* **2006,** *103* (42), 15309-15314.
14. Jakubowski, W.; Matyjaszewski, K., Activators regenerated by electron transfer for atom-transfer radical polymerization of (meth)acrylates and related block copolymers. *Angew Chem Int Ed Engl* **2006,** *45* (27), 4482-4486.
15. Matyjaszewski, K.; Dong, H.; Jakubowski, W.; Pietrasik, J.; Kusumo, A., Grafting from surfaces for "everyone": ARGET ATRP in the presence of air. *Langmuir* **2007,** *23* (8), 4528-4531.
16. Paterson, S. M.; Brown, D. H.; Chirila, T. V.; Keen, I.; Whittaker, A. K.; Baker, M. V., The synthesis of water-soluble PHEMA via ARGET ATRP in protic media. *Journal of Polymer Science Part A: Polymer Chemistry* **2010,** *48* (18), 4084-4092.
17. Enciso, A. E.; Fu, L.; Russell, A. J.; Matyjaszewski, K., A Breathing Atom-Transfer Radical Polymerization: Fully Oxygen-Tolerant Polymerization Inspired by Aerobic Respiration of Cells. *Angew Chem Int Ed Engl* **2018,** *57* (4), 933-936.
18. Narupai, B.; Page, Z. A.; Treat, N. J.; McGrath, A. J.; Pester, C. W.; Discekici, E. H.; Dolinski, N. D.; Meyers, G. F.; Read de Alaniz, J.; Hawker, C. J., Simultaneous Preparation of Multiple Polymer Brushes under Ambient Conditions using Microliter Volumes. *Angew Chem Int Ed Engl* **2018,** *57* (41), 13433-13438.
19. Wohlfahrt, G.; Witt, S.; Hendle, J.; Schomburg, D.; Kalisz, H. M.; Hecht, H. J., 1.8 and 1.9 angstrom resolution structures of the Penicillium amagasakiense and Aspergillus niger glucose oxidases as a basis for modelling substrate complexes. *Acta Crystallographica Section D-Biological Crystallography* **1999,** *55*, 969-977.
20. Gibson, Q. H.; Swoboda, B. E.; Massey, V., Kinetics and Mechanism of Action of Glucose Oxidase. *J Biol Chem* **1964,** *239*, 3927-3934.
21. Chapman, R.; Gormley, A. J.; Herpoldt, K.-L.; Stevens, M. M., Highly Controlled Open Vessel RAFT Polymerizations by Enzyme Degassing. *Macromolecules* **2014,** *47* (24), 8541-8547.
22. Schneiderman, D. K.; Ting, J. M.; Purchel, A. A.; Miranda, R.; Tirrell, M. V.; Reineke, T. M.; Rowan, S. J., Open-to-Air RAFT Polymerization in Complex Solvents: From Whisky to Fermentation Broth. *Acs Macro Letters* **2018,** *7* (4), 406-411.

23. Enciso, A. E.; Fu, L.; Lathwal, S.; Olszewski, M.; Wang, Z.; Das, S. R.; Russell, A. J.; Matyjaszewski, K., Biocatalytic "Oxygen-Fueled" Atom Transfer Radical Polymerization. *Angew Chem Int Ed Engl* **2018,** *57* (49), 16157-16161.
24. Vasileva, N.; Godjevargova, T., Study of the effect of some organic solvents on the activity and stability of glucose oxidase. *Materials Science and Engineering: C* **2005,** *25* (1), 17-21.
25. Balistreri, N.; Gaboriau, D.; Jolivalt, C.; Launay, F., Covalent immobilization of glucose oxidase on mesocellular silica foams: Characterization and stability towards temperature and organic solvents. *Journal of Molecular Catalysis B: Enzymatic* **2016,** *127*, 26-33.
26. Nakayama, Y.; Matsuda, T., In situ observation of dithiocarbamate-based surface photograft copolymerization using quartz crystal microbalance. *Macromolecules* **1999,** *32* (16), 5405-5410.
27. Döbbelin, M.; Arias, G.; Loinaz, I.; Llarena, I.; Mecerreyes, D.; Moya, S., Tuning Surface Wettability of Poly(3-sulfopropyl methacrylate) Brushes by Cationic Surfactant-Driven Interactions. *Macromolecular Rapid Communications* **2008,** *29* (11), 871-875.
28. Moya, S. E.; Brown, A. A.; Azzaroni, O.; Huck, W. T. S., Following Polymer Brush Growth Using the Quartz Crystal Microbalance Technique. *Macromolecular Rapid Communications* **2005,** *26* (14), 1117-1121.
29. Fantin, M.; Ramakrishna, S. N.; Yan, J.; Yan, W.; Divandari, M.; Spencer, N. D.; Matyjaszewski, K.; Benetti, E. M., The Role of Cu0 in Surface-Initiated Atom Transfer Radical Polymerization: Tuning Catalyst Dissolution for Tailoring Polymer Interfaces. *Macromolecules* **2018,** *51* (17), 6825-6835.
30. Sauerbrey, G., Verwendung Von Schwingquarzen Zur Wagung Dunner Schichten Und Zur Mikrowagung. *Zeitschrift Fur Physik* **1959,** *155* (2), 206-222.
31. Parlak, Z.; Biet, C.; Zauscher, S., Decoupling mass adsorption from fluid viscosity and density in quartz crystal microbalance measurements using normalized conductance modeling. *Measurement Science and Technology* **2013,** *24* (8), 085301.
32. Ramos, J. I.; Moya, S. E., Effect of the Density of ATRP Thiol Initiators in the Yield and Water Content of Grafted-From PMETAC Brushes. A Study by Means of QCM-D and Spectroscopic Ellipsometry Combined in a Single Device. *Macromolecular Chemistry and Physics* **2012,** *213* (5), 549-556.
33. Heeb, R.; Bielecki, R. M.; Lee, S.; Spencer, N. D., Room-Temperature, Aqueous-Phase Fabrication of Poly(methacrylic acid) Brushes by UV-LED-Induced, Controlled Radical Polymerization with High Selectivity for Surface-Bound Species. *Macromolecules* **2009,** *42* (22), 9124-9132.
34. Mouanda, B.; Bassa, E.; Deniau, G.; Jegou, P.; Viel, P.; Palacin, S., Comparison of two “grafting from” techniques for surface functionalization: Cathodic electrografting and surface-initiated atom transfer radical polymerization. *Journal of Electroanalytical Chemistry* **2009,** *629* (1-2), 102-109.

35. Jeon, H.; Schmidt, R.; Barton, J. E.; Hwang, D. J.; Gamble, L. J.; Castner, D. G.; Grigoropoulos, C. P.; Healy, K. E., Chemical patterning of ultrathin polymer films by direct-write multiphoton lithography. *J Am Chem Soc* **2011,** *133* (16), 6138-41.
36. Hosseiny, S.; van Rijn, P., Surface Initiated Polymerizations via e-ATRP in Pure Water. *Polymers* **2013,** *5* (4), 1229-1240.
37. Chernyy, S.; Iruthayaraj, J.; Ceccato, M.; Hinge, M.; Pedersen, S. U.; Daasbjerg, K., Elucidation of the mechanism of surface-initiated atom transfer radical polymerization from a diazonium-based initiator layer. *Journal of Polymer Science Part A: Polymer Chemistry* **2012,** *50* (21), 4465-4475.
38. Ma, H.; Textor, M.; Clark, R. L.; Chilkoti, A., Monitoring kinetics of surface initiated atom transfer radical polymerization by quartz crystal microbalance with dissipation. *Biointerphases* **2006,** *1* (1), 35-39.
39. Cheng, N.; Azzaroni, O.; Moya, S.; Huck, W. T. S., The Effect of [CuI]/[CuII] Ratio on the Kinetics and Conformation of Polyelectrolyte Brushes by Atom Transfer Radical Polymerization. *Macromolecular Rapid Communications* **2006,** *27* (19), 1632-1636.
40. He, J.; Wu, Y. Z.; Wu, J.; Mao, X.; Fu, L.; Qian, T. C.; Fang, J.; Xiong, C. Y.; Xie, J. L.; Ma, H. W., Study and application of a linear frequency-thickness relation for surface-initiated atom transfer radical polymerization in a quartz crystal microbalance. *Macromolecules* **2007,** *40* (9), 3090-3096.
41. Dekker, A. O.; Dickinson, R. G., Oxidation of ascorbic acid by oxygen with cupric ion as catalyst. *Journal of the American Chemical Society* **1940,** *62*, 2165-2171.
42. Ruiz, J. A., A.; Dominguez, M., Mechanism of L-ascorbicacid oxidation and dehydro-L-ascorbicacid reduction on a mercury electrode. *Can. J. Chem.* **1977,** *55*, 2799-2806.
43. Divandari, M.; Pollard, J.; Dehghani, E.; Bruns, N.; Benetti, E. M., Controlling Enzymatic Polymerization from Surfaces with Switchable Bioaffinity. *Biomacromolecules* **2017,** *18* (12), 4261-4270.
44. Lutz, J.-F., Polymerization of oligo(ethylene glycol) (meth)acrylates: Toward new generations of smart biocompatible materials. *Journal of Polymer Science Part A: Polymer Chemistry* **2008,** *46* (11), 3459-3470.
45. Wang, X.; Berger, R.; Ramos, J. I.; Wang, T.; Koynov, K.; Liu, G.; Butt, H.-J.; Wu, S., Nanopatterns of polymer brushes for understanding protein adsorption on the nanoscale. *RSC Adv.* **2014,** *4* (85), 45059-45064.
46. Li, S.; Chung, H. S.; Simakova, A.; Wang, Z.; Park, S.; Fu, L.; Cohen-Karni, D.; Averick, S.; Matyjaszewski, K., Biocompatible Polymeric Analogues of DMSO Prepared by Atom Transfer Radical Polymerization. *Biomacromolecules* **2017,** *18* (2), 475-482.
47. Emilsson, G.; Schoch, R. L.; Oertle, P.; Xiong, K.; Lim, R. Y. H.; Dahlin, A. B., Surface plasmon resonance methodology for monitoring polymerization kinetics and morphology changes of brushes—evaluated with poly(N -isopropylacrylamide). *Applied Surface Science* **2017,** *396*, 384-392.

48. Turbill, P.; Beugeling, T.; Poot, A. A., Proteins involved in the Vroman effect during exposure of human blood plasma to glass and polyethylene. *Biomaterials* **1996,** *17* (13), 1279-1287.
49. Luan, Y.; Li, D.; Wei, T.; Wang, M.; Tang, Z.; Brash, J. L.; Chen, H., "Hearing Loss" in QCM Measurement of Protein Adsorption to Protein Resistant Polymer Brush Layers. *Anal Chem* **2017,** *89* (7), 4184-4191.

TOC Image:

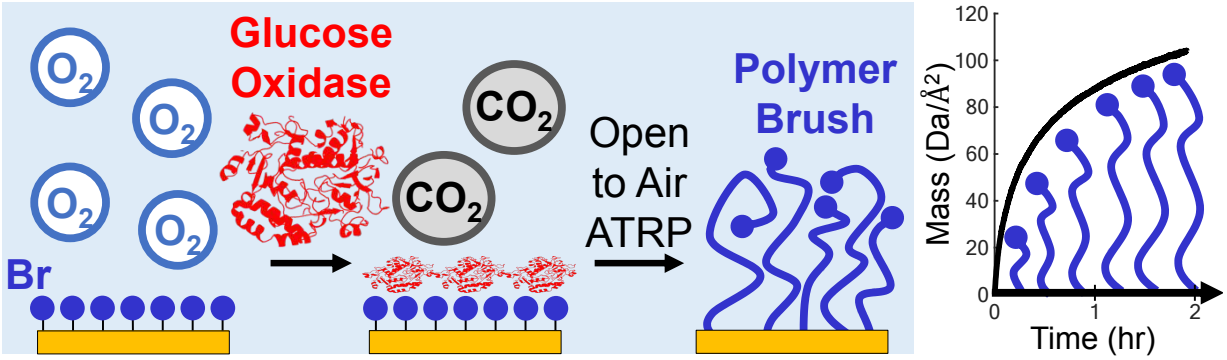
Glucose
Oxidase
O_2
O_2
O_2
O_2
CO_2
CO_2
Br
Open
to Air
ATRP
Polymer
Brush
Mass (Da/Å^2)
120
100
80
60
40
20
0
0
1
2
Time (hr)